

ARTICLES

 μ^-e^+ dilepton production in charged-current ν_μ interactions

N. J. Baker,* S. A. Kahn, M. J. Murtagh, N. P. Samios, and M. Tanaka
Brookhaven National Laboratory, Upton, New York 11973

C. Baltay,† E. R. Hyatt, S. Manly,† and R. Steiner‡
Columbia University, New York, New York 10027

P. F. Jacques, M. Kalelkar, R. J. Plano, and P. E. Stamer§
Rutgers University, New Brunswick, New Jersey 08903

(Received 21 June 1990; revised manuscript received 10 January 1991)

The production of μ^-e^+ dileptons by muon neutrinos is studied in a high-statistics bubble-chamber experiment. The experiment consisted of exposing the Fermilab 15-ft bubble chamber filled with a heavy Ne-H₂ mix to a wideband neutrino beam. In a total sample of $146\,700 \pm 11\,700$ charged-current interactions, 461 events with an e^+ ($P_{e^+} > 300$ MeV/c) and a μ^- are observed. The rate for μ^-e^+ dilepton production is measured to be $(0.42 \pm 0.06)\%$. The energy dependence of this rate is presented. The kinematic distributions for the μ^-e^+ events are consistent with charm production and subsequent semileptonic decay. A total of 60 K_S^0 and 31 Λ^0 decays were observed in the μ^-e^+ event sample. The measured rates for neutral-strange-particle production are 0.78 ± 0.12 K^0/\bar{K}^0 's and 0.19 ± 0.04 Λ^0 's per μ^-e^+ event. Finally, rates for Λ_c^+ , D^0 , and D^+ production in charged-current ν_μ interactions are derived. They are found to be $(4^{+10}_{-2})\%$, $(1.7^{+0.5}_{-0.2})\%$, and $(1.3^{+0.4}_{-0.2})\%$, respectively.

I. INTRODUCTION

The results of a study of μ^-e^+ dilepton production in charged-current ν_μ interactions in the 15-ft bubble chamber at Fermilab are presented. The data set used for this analysis is twice as large as that in our most recent publication on this subject.¹ It also represents an increase in statistics of almost an order of magnitude over previously published similar works from other experiments.

The production of dileptons in neutrino interactions was first reported in 1975.² Since then these events have been studied extensively in both counter experiments³ and bubble chambers.^{1,4} Counter experiments have accumulated large samples of $\mu^-\mu^+$ events, while bubble chambers have produced smaller samples of μ^-e^+ and $\mu^-\mu^+$ events and have provided details of the accompanying hadronic system. The predominant source of ν -induced dileptons has been shown to be the production and subsequent semileptonic decay of charmed particles. Therefore, the emphasis in this paper is not to establish the origin of these events but rather to investigate the phenomenon of charm production by neutrinos.

In Sec. II of this paper, some experimental details are presented. Section III gives a discussion of the data selection. The backgrounds and corrections to the data are described in Sec. IV. The results are given in Sec. V, which is divided into four subsections. Section V A contains a discussion of the kinematic distributions of the μ^-e^+ events. In Sec. V B the μ^-e^+ production rate is calculated. Strange-particle production in these events is examined in Sec. V C. Finally in Sec. V D, the produc-

tion of charmed particles in μ^-e^+ dilepton events is discussed. The study is summarized in Sec. VI.

II. EXPERIMENTAL PROCEDURE

The data used in this analysis come from experiment E53 at Fermilab. In this experiment, the 15-ft bubble chamber was exposed to a horn-focused wide-band neutrino beam. There were two separate runs, referred to in this paper as E53A and E53B, respectively. The full E53 data sample was used in this analysis.

The neutrino beam was generated by 400-GeV protons incident on a target of Al₂O₃ during E53A and BeO during E53B. Positively charged secondary particles from the production target were focused by two magnetic horns in E53A and by a single horn in E53B. After focusing, the secondaries were allowed to decay in a 400-m decay space. The bubble chamber was separated from this decay space by 1 km of earth, which absorbed all particles except the beam neutrinos. The resulting muon-neutrino spectrum peaked at 20 GeV and extended out to approximately 200 GeV.

The bubble chamber was filled with a heavy Ne-H₂ mixture (64 at. % neon). The 40-cm radiation length in this mixture allowed for easy identification of electrons. The interaction length in this liquid is 125 cm, short enough to provide good muon-hadron separation.

The bubble chamber was roughly spherical with a diameter of 3.7 m and a total target weight of 25 tons. A 30-kG magnetic field uniform to 15% was present throughout the chamber volume. Events were photographed with three cameras. A total of approximately

400 000 photographs were taken in the two runs. The estimated number of ν_μ charged-current events in the film is 200 000, split about evenly between E53A and E53B.

III. DATA SELECTION

In order to identify μ^-e^+ dilepton candidates, the film was scanned for all events with an e^+ coming from the vertex with a momentum greater than 300 MeV/c. To be identified as an e^+ , the track was required to exhibit at least two signatures characteristic of positrons in a heavy liquid. These signatures are (1) bremsstrahlung with a $\gamma \rightarrow e^+e^-$ conversion, (2) spirialization, (3) production of a δ ray with energy comparable to the primary track, and (4) annihilation with two $\gamma \rightarrow e^+e^-$ conversions. The selected events were measured and processed through the geometrical-reconstruction program TVGP.⁵ In addition, the measured neutral-strange-particle decays (V^0 s) and γ conversions were passed through the kinematic-fitting program SQUAW. For each measured V^0 , SQUAW attempted to make constrained fits to the vertex for the following hypotheses: $K_S^0 \rightarrow \pi^+\pi^-$, $\Lambda^0 \rightarrow p\pi^-$, $\bar{\Lambda}^0 \rightarrow \pi^+\bar{p}$, and $\gamma p \rightarrow pe^+e^-$. For each measured γ , fits to the last hypothesis only were attempted. Only those fits with a χ^2 per degree of freedom less than five were considered during later stages of the analysis.

After being scanned, measured, and reconstructed, each event containing an e^+ track was carefully edited by a physicist. At this stage the event reconstruction was checked and obvious background events were removed. In addition, fiducial volume cuts were made to remove events more than 125 cm above or below the midplane of the bubble chamber, events within 15 cm of the wall of the bubble chamber, and events within 75 cm of the back wall of the chamber. The first cut removed events close to the cameras and those near the bottom of the chamber. The large bubble size on the film for events close to the cameras and the loss of resolution for interactions far from the cameras prohibited accurate measurements for these events. The second cut decreased the possibility that the incoming neutral particle inducing the event was from an interaction in the bubble-chamber wall. The final cut was made to exclude events near the back wall of the chamber. This was necessary to ensure good particle identification, to allow room for neutral particles to decay or interact, to reduce the momentum-measurement error on each charged track, and to reduce the chances of mistaking a hadron for a muon. The fiducial volume had a weight of 17 tons. The fiducial-volume cuts removed approximately one-quarter of the events, leaving 685 events with an e^+ .

Of the 685 events containing an e^+ , 461 also had at least one leaving negative (L^-) track. The highest-momentum L^- track in each event was interpreted as a μ^- leaving the chamber. Thus, the 461 events with both a positron and an L^- track constituted the raw μ^-e^+ event sample.

The normalization sample of charged-current ν_μ interactions came from a scan of approximately 1.3% of the pictures scattered throughout the film. During this scan, the scanners measured any event in the bubble

chamber induced by a neutral particle traveling in the ν beam direction.

Charged-current ν_μ interactions (ν_μ CC) were defined to be events inside the fiducial volume which had $E_\nu > 10$ GeV and at least one negative leaving track, where E_ν is defined to be the total visible energy of the event corrected for missing neutral energy as described in Sec. V A. In addition, the fractional energy transfer to the hadronic system,

$$y = \frac{E_\nu - E_\mu}{E_\nu},$$

was required to be less than 0.85, where the muon was assumed to be the highest-momentum L^- track. The energy cut was necessary to eliminate the background from neutrons and neutral-strange particles. The y cut reduced the neutral-current and charged-current $\bar{\nu}_\mu$ contamination. Events with high y had a relatively low lepton momentum and there was a significant background from the neutral-current and charged-current $\bar{\nu}_\mu$ events with hadrons that left the chamber (the so-called hadron punchthrough background).

Similarly, the charged-current $\bar{\nu}_\mu$ ($\bar{\nu}_\mu$ CC) sample was defined to be those events inside the fiducial volume with $E_\nu > 10$ GeV, a leaving positive (L^+) track, $y < 0.85$, and no L^- track. Those events not satisfying the ν_μ CC- or $\bar{\nu}_\mu$ CC-event requirements were placed in the "neutral-current" (NC) sample. This is somewhat of a misnomer since no attempt was made to isolate true neutral-current events in this analysis. Having defined the various categories in the manner described above, the normalization sample yielded 1501 ν_μ CC candidates, 99 $\bar{\nu}_\mu$ CC candidates, and 499 NC candidates.

IV. BACKGROUNDS AND CORRECTIONS

The primary backgrounds in the μ^-e^+ sample come from charged-current $\bar{\nu}_e$ interactions with an L^- track and charged-current ν_μ interactions with an asymmetric Dalitz pair or close-in asymmetric γ conversion. Other sources of background such as leptonic decays of hadrons or accidental misidentification of a hadron as a positron are negligible.

The background due to charged-current $\bar{\nu}_e$ interactions with an L^- track (so-called $\bar{\nu}_e$ punchthrough) was estimated from the sample of events with an e^+ but no L^- track. These events are mostly charged-current $\bar{\nu}_e$ interactions and are referred to as the $\bar{\nu}_e$ CC sample. The background in the μ^-e^+ sample was calculated by assigning N weights to each event in the $\bar{\nu}_e$ CC sample with N interacting negative (I^-) tracks. These weights represented the probability that any of the N I^- tracks leave the chamber mimicking a muon. Each weight was corrected for those $\bar{\nu}_e$ charged-current events already lost from the sample (i.e., already background in the μ^-e^+ sample) by dividing the weight by the probability that none of the I^- tracks leave the chamber. The sum of these weights for all the $\bar{\nu}_e$ CC events represented the number of background events in the μ^-e^+ sample from this source. This calculation yielded a value for this

background of 62 ± 12 events or $(13 \pm 3)\%$ of the total μ^-e^+ sample in the two runs.

In addition to correcting the μ^-e^+ rate, it was necessary to correct the μ^-e^+ kinematic distributions for the $\bar{\nu}_e$ punchthrough background. This was done by using a generalization of the calculation used to correct the rate. In this case, it was necessary to calculate a weight for each I^- track in the $\bar{\nu}_e$ CC sample. This weight represented the probability that the given I^- track leave the chamber while none of the other I^- tracks with greater momentum associated with the same event leave. This selected the topology where the given I^- track is mistaken to be a μ^- , and the event becomes part of the background in the μ^-e^+ sample. The weight was corrected as above for events already lost from the $\bar{\nu}_e$ sample. Kinematic distributions were created assuming each of the I^- tracks to be a muon. The weight associated with a given I^- track was used to weight that entry in the distributions. These distributions were subtracted as background from the μ^-e^+ kinematic distributions.

The background due to charged-current ν_μ interactions with an asymmetric Dalitz pair or a close-in asymmetric γ conversion was experimentally determined. This was done by measuring the momentum distribution of samples of Dalitz pairs and γ conversions and folding in the probability for them to convert asymmetrically. An asymmetric conversion is one where one prong of the e^-e^+ pair has a momentum less than 5 MeV/c. This corresponds to a radius of curvature at the lower limit of what the scanners can reliably see (~ 0.5 cm). It was determined that there are 1.3×10^{-4} asymmetric pairs per charged-current ν_μ event where the momentum of the visible prong is greater than 300 MeV/c. This corresponds to a background of 19 ± 6 events in the μ^-e^+ sample. A smaller background comes from neutral-current events with both an asymmetric pair and a negative hadron that leaves the chamber. The background due to this source is estimated to be 2 ± 1 events. Thus, the total background in the 461 μ^-e^+ events is estimated to be 83 ± 13 events or $(18 \pm 3)\%$.

After background subtraction, there are 378 ± 26 μ^-e^+ events inside the fiducial volume (189 ± 16 in E53A and 189 ± 20 in E53B). To determine the actual number of μ^-e^+ events produced in this experiment, it is necessary to correct for various losses and inefficiencies. The scanning efficiency was determined to be 75% (77%) in E53A (E53B) by rescanning portions of the film. The e^+ identification efficiency is the probably that an e^+ have two identifying signatures. This probability was determined as a function of momentum by examining converted γ 's in the bubble chamber. The e^+ identification efficiency is $(94 \pm 4)\%$. The confused event loss arose from events that were too messy to measure or to determine the presence or absence of an e^+ . It was estimated to be $(10 \pm 5)\%$ by examining scan and edit notes. In addition, there is a miscellaneous loss estimated to be $(5 \pm 5)\%$. This is due to things such as stopping muons and misidentifying the e^+ as a member of a Dalitz pair or γ conversion because it has a small opening angle with a leaving negative hadron. There is no correction made for the 300-MeV/c cut on the positron momentum. Given

the low-momentum cut in this experiment, the need for such a correction is small. Table I summarizes the corrections for losses and efficiencies for the μ^-e^+ sample. The corrected number of μ^-e^+ events (N_c) is given by

$$N_c = N_o \frac{1}{C_1 C_2 C_3 C_4},$$

where N_o is the observed number of events and the C_i are as defined in Table I. The total corrected number of μ^-e^+ events in this experiment is 618 ± 74 (313 ± 43 in E53A and 305 ± 46 in E53B). It should be noted that for this result and many of the others presented in this paper the error due to the systematic corrections is as large or larger than the one due to statistics.

As described in Sec. III, the normalization sample yielded 1501 charged-current ν_μ candidates. However, even after the y cut, there remains a small contamination of neutral-current and charged-current $\bar{\nu}_\mu$ events with a negative leaving hadron in the ν_μ CC sample. This contamination has to be taken into account when calculating the final number of charged-current ν_μ events.

The punchthrough background in the ν_μ CC sample is handled in a statistical manner. The data are used to construct weighted simulated events that yield estimates for the corrections and backgrounds in the rate. For example, the NC punchthrough into the ν_μ CC sample is estimated by constructing a new sample of events from those events in the NC sample that have at least one interacting negative track that would pass the y cut if it were to leave the bubble chamber. Each of the events in this new sample is weighted by the probability that the negative track leave the chamber and corrected for those events missing from the NC sample because they are identified as ν_μ CC events. The rate of these newly created events is subtracted from that of the ν_μ CC sample as background. Further details of this work can be found in other publications of this collaboration.⁶ After the cuts and background subtraction described above there are 1439 ν_μ charged-current interactions in the sample (834 ± 29 in E53A and 605 ± 25 in E53B).

The normalization sample of charged-current ν_μ events must be corrected for the energy and y cuts, as well as for event confusion and scanning efficiency. The loss due to the 10-GeV energy cut was estimated by using the charged-current ν_μ interaction event spectrum predicted from a Monte Carlo simulation of the neutrino beam. This Monte Carlo program is described in detail else-

TABLE I. Acceptance corrections and efficiencies for the μ^-e^+ dilepton events.

Correction	
C_1 , scan efficiency	0.75 ± 0.05 (E53A) 0.77 ± 0.05 (E53B)
C_2 , confused event	0.90 ± 0.05
C_3 , e^+ identification efficiency	0.94 ± 0.04
C_4 , miscellaneous losses	0.95 ± 0.05

TABLE II. Acceptance corrections and efficiencies for the charged-current ν_μ events.

Correction	
$C_1, E_\nu > 10 \text{ GeV}$	$1.08 \pm 0.01 \text{ (E53A)}$
	$1.06 \pm 0.01 \text{ (E53B)}$
$C_2, y < 0.85$	1.12 ± 0.01
$C_3, \text{ scan efficiency}$	0.90 ± 0.05
$C_4, \text{ confused event}$	0.95 ± 0.05

where.⁶ The loss due to the y cut was determined using the Buras and Gaemers parametrization of $\sigma(x,y)$ for ν_μ charged-current interactions with radiative corrections.⁷ The confused event loss arises from events that are too messy to measure. It was estimated by examining scan and edit notes. The scanning efficiency for these events was determined by rescanning part of the film. The corrected number of charged-current ν_μ interactions (N_c) is given by

$$N_c = N_o \frac{C_1 C_2}{C_3 C_4},$$

where N_o is the observed number of events and the C_i are as defined in Table II. After applying these corrections and scaling the number up to represent the total data sample, there are $146\,700 \pm 11\,700$ charged-current ν_μ interactions inside the fiducial volume in this experiment ($76\,100 \pm 6900$ in E53A and $70\,600 \pm 6400$ in E53B).

V. RESULTS

A. Kinematics

The incident neutrino energy (E_ν) for the $\mu^- e^+$ events is shown in Fig. 1. Both the raw and background-subtracted distributions are given. The background subtraction is described in Sec. IV. Only a few error bars are shown on the plot for simplicity. The errors are smooth and well behaved. (The same is true for most of the other figures in this paper.) E_ν has been corrected for missing neutral particles using a simple method developed in a narrow-band neutrino-beam experiment by the same group in the same chamber with the same heavy Ne-H₂ fill.⁸ Such a correction can be developed in a narrow-band beam because in this type of beam there is a well-understood relation between the incident neutrino energy and the event location in the detector. The energy-correction method is summarized as follows:

$$E_h < 20 \text{ GeV}, \quad E_h^c = 1.11 E_h;$$

$$20 \leq E_h \leq 100 \text{ GeV}, \quad E_h^c = (0.003 E_h + 1.05) E_h;$$

$$E_h > 100 \text{ GeV}, \quad E_h^c = 1.35 E_h,$$

where E_h is the sum of energy of the visible charged and converted neutral particles judged to be associated with the hadronic sector of the event plus 3 GeV, E_h^c is the hadronic energy corrected for missing neutral particles, and E_ν is the sum of E_h^c and the energy of the primary final-state lepton. The additional 3 GeV in E_h is an attempt to

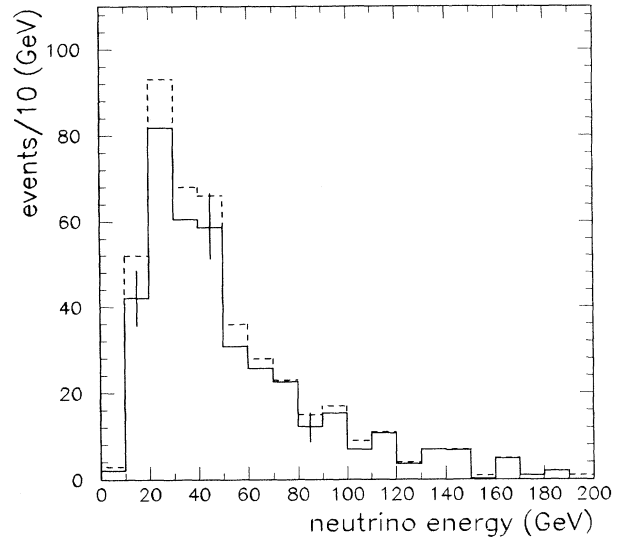


FIG. 1. E_ν spectrum for $\mu^- e^+$ events. The dashed line gives the distribution of the raw data, and the solid line shows the distribution after background subtraction.

statistically take into account the loss of energy due to the neutrino present in semileptonic charm decay. It is necessary to include this because the overall event energy correction described here (not including the additional 3 GeV) was developed using ordinary ν_μ charged-current events, most of which do not contain a semileptonic charm decay. The value of 3 GeV was chosen after examining the positron energy spectrum which is expected to be similar to that for the missing semileptonic decay neutrino.

Figures 2 and 3 give the muon and positron momentum distribution for the $\mu^- e^+$ events, respectively. Note

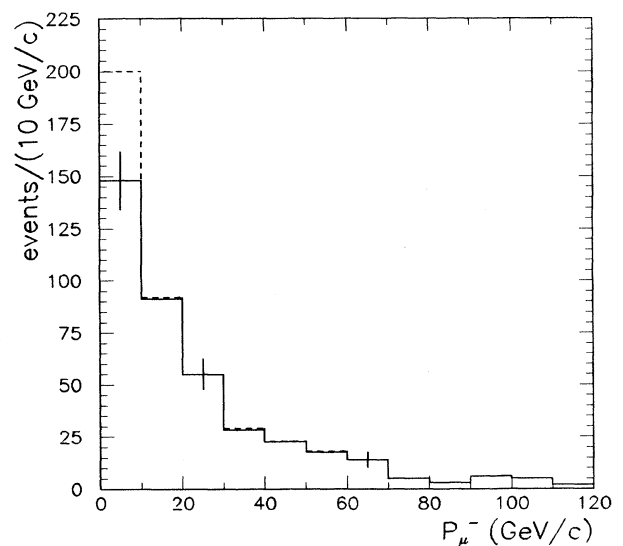


FIG. 2. P_μ^- distribution for $\mu^- e^+$ events. The dashed and solid lines represent the raw and background-subtracted data, respectively.

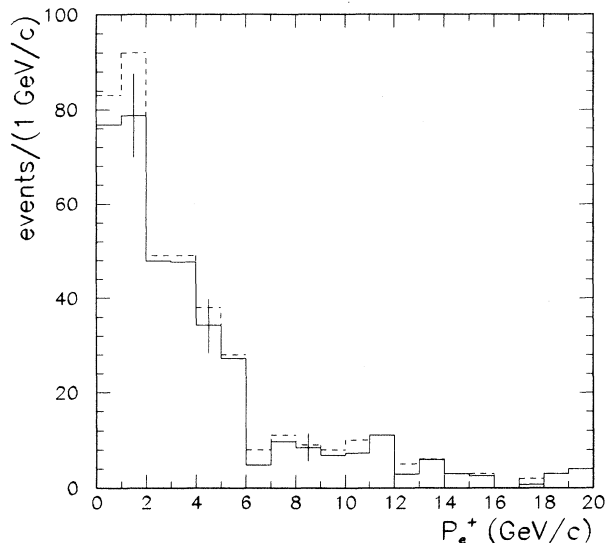


FIG. 3. P_{e^+} distribution for $\mu^- e^+$ events. The dashed and solid lines represent the raw and background-subtracted data, respectively.

the difference in the momentum scales. The hard μ^- momentum and the soft e^+ momentum are consistent with the hypothesis that the latter lepton comes from the production of charm and its subsequent semileptonic decay in a ν_μ charged-current interaction. The momenta are obtained from measurements of curvature in the magnetic field. This method gives reasonable results for positrons with such low momenta.⁹ Also note that most of the positrons have momenta less than 4 GeV/c, below where most of the counter experiments make their lepton-momentum cuts in studies of opposite-sign dileptons.

Evidence that the positron is associated with the hadronic part of the event is given in Figs. 4(a)–4(c). Here the opening angle between the projections of selected vectors onto the plane normal to the neutrino direction are plotted. In Fig. 4(a) the angle between the projection of the momentum vector of the hadronic system (all tracks except the μ^- and the e^+) and that of the muon is seen to peak at 180° . Similarly, the corresponding angle between the muon and the positron peaks at 180° , as seen in Fig. 4(b). In contrast, the angle between the projection of the momentum vector of the hadronic system and that of the positron is relatively flat as shown in Fig. 4(c). These distributions are clearly consistent with the hypothesis that the e^+ comes from the production and subsequent semileptonic decay of charm in the hadronic sector of the $\mu^- e^+$ events.

The kinematic distributions of the variables

$$Q^2 = 2E_\nu E_\mu (1 - \cos\theta_\mu),$$

$$x = \frac{Q^2}{2m_p \nu}, \quad y = \frac{\nu}{E_\nu},$$

and

$$W^2 = m_p^2 + 2m_p \nu - Q^2,$$

where $\nu = E_\nu - E_\mu$ and m_p is the proton mass, are shown in Figs. 5(a)–5(d). The x distribution is the most interesting. In the standard quark-parton model, x represents the fraction of the target nucleon's momentum carried by the struck quark. For charged-current neutrino interactions that do not produce charm, the x distribution is primarily a d -quark momentum distribution. This is because the neutrino predominantly interacts with a d quark, $\nu_\mu d \rightarrow \mu^- u X$, with a strength proportional to $\cos^2\theta_C \sim 0.95$ (where θ_C is the Cabibbo angle). It can also interact with a sea s quark, $\nu_\mu s\bar{s} \rightarrow \mu^- u\bar{s} X$. However, in this case the interaction is Cabibbo suppressed; i.e., it occurs with a strength proportional to $\sin^2\theta_C \sim 0.05$. In neutrino interactions that produce charm, the c quark is produced from a d quark with a strength proportional to $\sin^2\theta_C$ ($\nu_\mu d \rightarrow \mu^- c X$) or from a sea s quark with a strength proportional to $\cos^2\theta_C$ ($\nu_\mu s\bar{s} \rightarrow \mu^- c\bar{s} X$). Since the d -quark contribution is Cabibbo suppressed in this case, the x distribution is different from that where charm is not produced. Also, it should be noted that the kinematic distributions are somewhat different than might be expected in the simple quark-parton model with massless quarks because the mass of the charm quark is not negligible.¹⁰

B. $\mu^- e^+$ production rate

Using the corrected numbers of $\mu^- e^+$ and normalization events from Sec. IV the overall dilepton rate was calculated to be

$$\frac{\nu_\mu \text{Ne} \rightarrow \mu^- e^+ X}{\nu_\mu \text{Ne} \rightarrow \mu^- X} = (0.42 \pm 0.06)\%.$$

This number represents the rate for both runs combined. The samples were combined in quadrature after making the unshared systematic corrections and prior to correcting for shared systematics. The $\mu^- e^+$ production rate is given as a function of energy in Fig. 6. The background was subtracted bin by bin in the derivation of these rates. Global systematic corrections were used. Many of the systematic corrections do not vary with energy. Those that do should vary only a small amount over the energy range relevant for this experiment. The errors on the systematic corrections are large enough to take this into account. The bin-by-bin rate derivation is given in Table III. Published rates from some other experiments are given as well in Fig. 6 for comparison.^{11–15} The rates shown in this figure are either corrected for the lepton-momentum cuts or have very-low-momentum cuts (< 300 MeV/c). Therefore, Fig. 6 represents a charm-excitation curve for charged-current ν_μ interactions.

Counter experiments examining opposite-sign dilepton production require the lepton momenta to be greater than 4 GeV/c. When the same cuts are applied to the data in this experiment, the overall $\mu^- e^+$ production rate becomes $(0.14 \pm 0.02)\%$. This rate is given as a function of energy in Fig. 7. Published rates from other experiments are provided for comparison.^{12, 13, 16, 17}

The rate for opposite-sign dilepton production is relatively insensitive to a cut on the leading-lepton momentum due to the fact that any such cut is applied to both

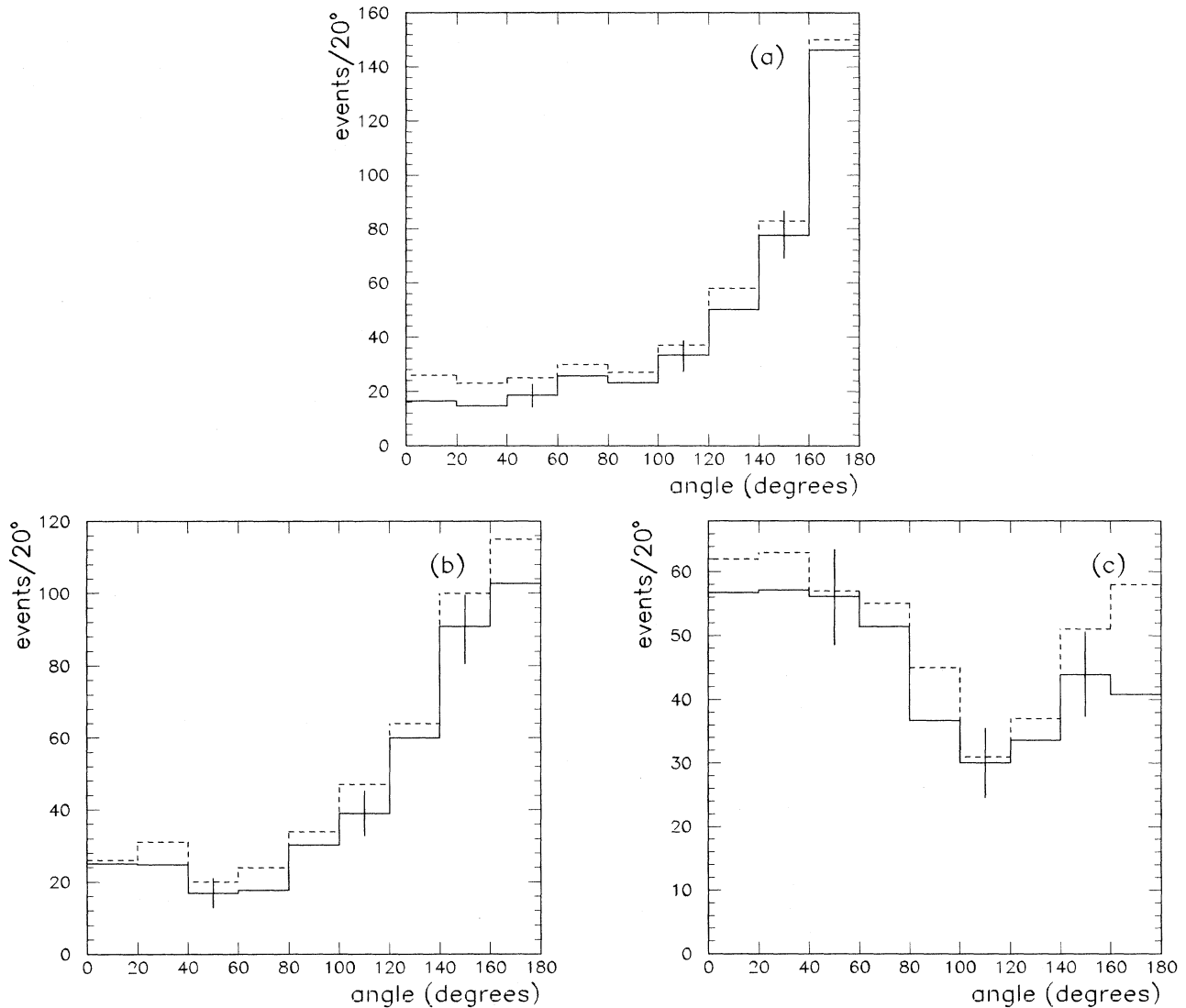


FIG. 4. Kinematic distributions for μ^-e^+ events. (a) The angle between the transverse momenta of μ^- and the hadronic system is shown. (b) The angle between the transverse momenta of μ^- and e^+ is given. (c) The angle between the transverse momenta of the hadronic system and e^+ . Raw and background-subtracted distributions are represented by dashed and solid lines, respectively.

the dilepton and charged-current samples. However, it is sensitive to a momentum cut on the second lepton. In this experiment, the only cut on lepton momenta is a 300-MeV/ c cut on the e^+ momentum imposed at the scanning stage. The rate was not corrected for the positron-momentum cut because of the relatively small size of the cut and the model-dependent uncertainties implicit in making such a correction. In counter experiments, where the second-lepton-momentum cut is much higher (≥ 4 GeV/ c), it is necessary to correct the data by a model-dependent Monte Carlo calculation.^{11,12} As can be seen in Figs. 6 and 7, this correction is very important at low energies. It should be noted that the rates shown in these plots are uncorrected for slow rescaling.¹⁰

C. Strange-particle production

A search for neutral-strange-particle decays yielded 92 V^0 's in the 461 μ^-e^+ events. Each of these V^0 's fit to at least one of the following hypotheses: $K_S^0 \rightarrow \pi^+\pi^-$, $\Lambda^0 \rightarrow p\pi^-$, or $\bar{\Lambda}^0 \rightarrow \pi^+\bar{p}$. Only those fits with a χ^2 per degree of freedom less than five were considered. In addition, the V^0 's were required to be farther than 1 cm from the neutrino vertex since the scanning efficiency was poor for V^0 's within 1 cm and to be farther than 10 cm from any wall to lessen the background from interactions in the walls of the bubble chamber. Finally, the calculated lifetime for each V^0 was required to be less than six proper lifetimes for that particular particle. Some V^0 's fit well

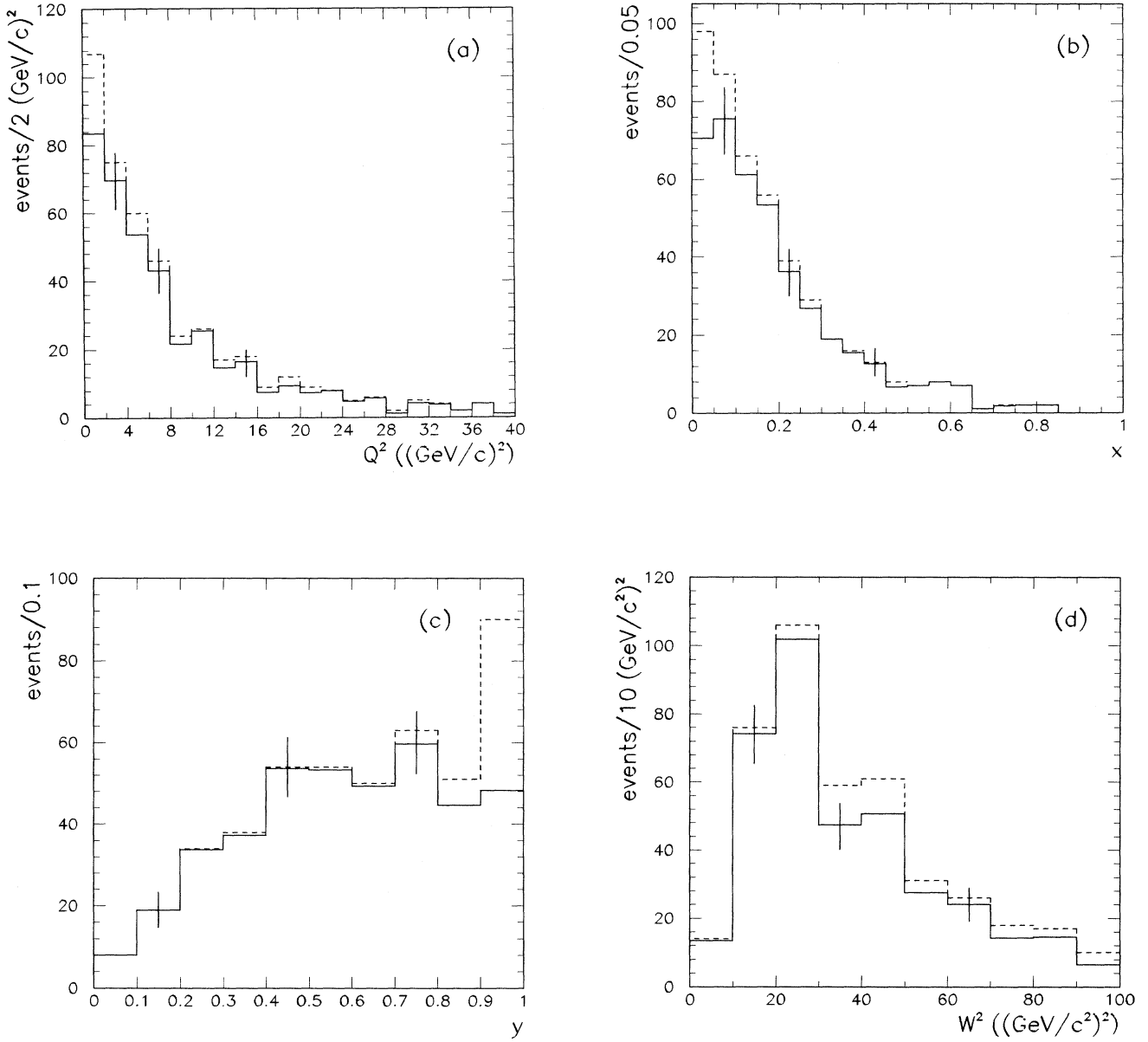


FIG. 5. Kinematic distributions for μ^-e^+ events. The plotted variables are (a) Q^2 , (b) x , (c) y , and (d) W^2 . The dashed lines give the distributions of the raw data, and the solid lines show the distribution after background subtraction.

to more than one hypothesis. The resolution of these ambiguous fits is discussed in detail in previous publications.^{1,18} After resolution of these ambiguities, there were a total of 60 $K_S^0 \rightarrow \pi^+\pi^-$ (36 in E53A, 24 in E53B), 31 $\Lambda^0 \rightarrow p\pi^-$ (17 in E53A, 14 in E53B), and 1 $\bar{\Lambda}^0 \rightarrow \pi^+\bar{p}$ (in E53A) observed in the μ^-e^+ sample.

To calculate the K^0 and Λ^0 production rates it was necessary to correct the observed number of K_S^0 's and Λ^0 's for backgrounds, losses, inefficiencies, and branching ratios. The backgrounds come from ν_μ charged-current interactions with an asymmetric Dalitz pair or close-in γ conversion and a V^0 and from $\bar{\nu}_e$ charged-current in-

teractions with hadron punchthrough and a V^0 . The backgrounds were calculated using previous reports of V^0 production in charged-current ν_μ and $\bar{\nu}_e$ interactions in this experiment.^{6,18} The total background was estimated to be 1.4 ± 0.4 K_S^0 's and 1.3 ± 0.4 Λ^0 's. The appropriate corrections for losses and efficiencies were determined in a study of V^0 production by muon neutrinos in this experiment.¹⁸ They are summarized in Table IV. The corrected number of V^0 's (N_c) was given by

$$N_c = N_0 \frac{C_1 C_2 C_3 C_4 C_5 C_9}{C_6 C_7 C_8},$$

TABLE III. μ^-e^+ rates as a function of the neutrino energy.

Energy bin (GeV)	μ^-e^+ events uncorrected background subtracted	μ^-e^+ corrected	ν_μ charged-current interactions	μ^-e^+ rate per ν_μ interaction
E53A				
0-25	40±8	66±15	30 590±2890	(0.22±0.06)%
25-50	74±9	123±21	26 620±2590	(0.46±0.09)%
50-100	52±7	86±15	13 690±1540	(0.63±0.13)%
100-200	20±5	33±9	4 480±690	(0.74±0.23)%
E53B				
0-25	29±9	47±15	25 450±2600	(0.18±0.06)%
25-50	80±11	129±23	22 690±2360	(0.57±0.12)%
50-100	52±8	84±15	14 870±1760	(0.56±0.12)%
100-200	21±5	33±9	6 720±1030	(0.49±0.15)%
E53A + E53B				
0-25		113±22	56 040±4920	(0.20±0.04)%
25-50		252±34	49 310±4390	(0.51±0.08)%
50-100		170±24	28 560±2800	(0.60±0.10)%
100-200		67±14	11 200±1370	(0.60±0.15)%

where N_o is the observed number and the C_i are defined in Table IV. Note that the branching ratio for K^0 's includes a factor of 2 for K_L , so that the rates presented here are for $K^0 + \bar{K}^0$. After corrections, there were 293 ± 39 K^0 's (177 for E53A, 116 for E53B) and 72 ± 15 Λ^0 's (40 for E53A, 32 for E53B) in the full-data sample. Combining both runs and correcting for systematic errors gives the following relative rates for neutral-strange-particle production in the μ^-e^+ events:

$$\frac{\nu_\mu \text{Ne} \rightarrow \mu^- e^+ K^0 X}{\nu_\mu \text{Ne} \rightarrow \mu^- e^+ X} = 0.78 \pm 0.12,$$

$$\frac{\nu_\mu \text{Ne} \rightarrow \mu^- e^+ \Lambda^0 X}{\nu_\mu \text{Ne} \rightarrow \mu^- e^+ X} = 0.19 \pm 0.04.$$

The rates are shown as a function of energy in Fig. 8.

In general, enhanced strange-particle production is expected for neutrino interactions that produce charm. In these interactions strange particles can arise either from the decay of the c quark to an s quark, which is Cabibbo

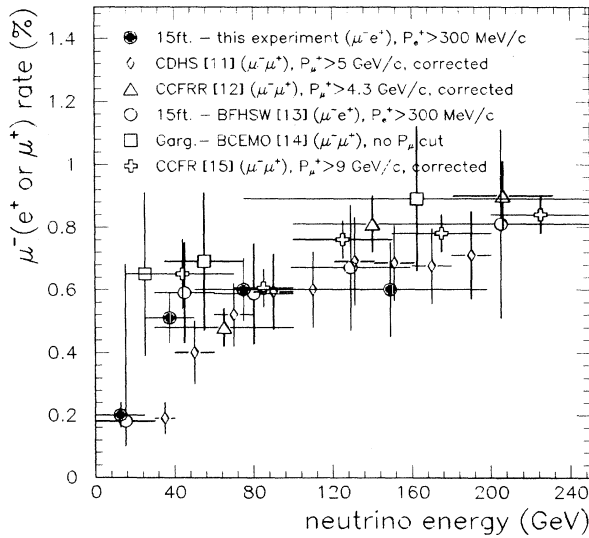


FIG. 6. Ratio of μ^-l^+ events to charged-current ν_μ events as a function of incident neutrino energy. For the rates in this plot, the lepton-momentum cuts are either very small or the data are corrected for the cuts.

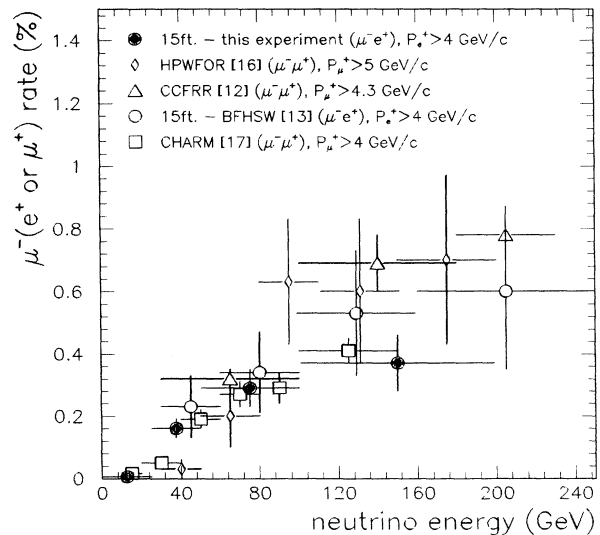


FIG. 7. Ratio of μ^-l^+ events to charged-current ν_μ events as a function of incident neutrino energy. The lepton momenta are greater than 4 GeV/c.

TABLE IV. Correction factors for V^0 production.

Corrections	K^0	Λ^0
C_1 , geometric detection efficiency	1.147 ± 0.004	1.117 ± 0.003
C_2 , interaction before decay	1.17 ± 0.02	1.16 ± 0.03
C_3 , low lifetime loss	1.15 ± 0.02	1.11 ± 0.02
C_4 , slow decay prong	1.03 ± 0.01	1.06 ± 0.01
C_5 , fake fits	0.95 ± 0.02	0.95 ± 0.02
C_6 , random scan efficiency	0.95 ± 0.02	0.95 ± 0.02
C_7 , reconstruction efficiency	0.96 ± 0.02	0.96 ± 0.02
C_8 , branching ratio	0.343 ± 0.001	0.642 ± 0.005
C_9 , ambiguity resolution	1.04 ± 0.02	0.97 ± 0.02

avored, or from a leftover sea \bar{s} quark. Thus, when charm is produced from a d quark, there should be one strange particle produced, and when it is produced from a sea s quark, there should be two. To examine this experimentally, the observation of 92 V^0 's in the 461 μ^-e^+ events can be contrasted to the neutral-strange-particle production in ν_μ charged-current events, which was studied previously in this experiment.¹⁸ Rates of 0.037 ± 0.001 K_S^0 's and 0.029 ± 0.001 Λ^0 's per charged-current event have been measured, respectively. In 461 events one would expect 17 ± 1 K_S^0 's and 14 ± 1 Λ^0 's to be produced. The excess of 43 ± 8 K_S^0 's and 17 ± 6 Λ^0 's can be attributed to the enhanced strange-particle production in events containing charmed particles. Correcting the excess strange particles for cuts and efficiencies as described above yields an excess of 215 ± 40 K^0 's and 41 ± 14 Λ^0 's in the μ^-e^+ sample. Assuming the number of charged strange particles is the same as the number of neutral strange particles (i.e., the number of $K^+ =$ number of K^0 , etc.) and using the background-corrected number of μ^-e^+ events gives

$$\frac{\text{strange-particle excess}}{\mu^-e^+ \text{ event}} = \frac{512 \pm 84}{378 \pm 26} = 1.35 \pm 0.24$$

as the number of strange particles per μ^-e^+ event due to charm production.

The number of strange particles per μ^-e^+ event due to charm production in the quark-parton model can be estimated using the ratio of charm production from s

quarks to that from d quarks. The s/d -quark charm-production ratio can be estimated from the measured value of

$$\eta_s = \frac{2S_0}{U_0 + D_0},$$

where S_0 , U_0 , and D_0 represent the integral of the quark-momentum densities, i.e.,

$$S_0 = \int_0^1 s(x) dx.$$

Using the fact that Ne is an isoscalar target and assuming the difference between the u - and d -quark momentum distributions to be small,

$$\eta_s = \frac{2S_0}{U_0 + D_0} \sim \frac{S_0}{D_0}.$$

Therefore the s/d -quark charm-production ratio (S/D) is given by

$$S/D = \eta_s \frac{\cos^2 \theta_C}{\sin^2 \theta_C}.$$

Taking $\eta_s = 0.06 \pm 0.01$ as measured by counter experiments^{11,12,15} and $\cos^2 \theta_C / \sin^2 \theta_C = 19.8 \pm 0.4$ (Ref. 19) gives $S/D = 1.2 \pm 0.2$. This value can be used to calculate the number of strange particles (SP's) per μ^-e^+ event arising from charm production as follows:

$$(d \rightarrow c) \cos^2 \theta_C \left[1 \frac{\text{SP}}{\text{event}} \right] + (s \rightarrow c) \left[\cos^2 \theta_C \left[2 \frac{\text{SP}}{\text{event}} \right] + \sin^2 \theta_C \left[1 \frac{\text{SP}}{\text{event}} \right] \right] = 1.40 \pm 0.011,$$

where $(d \rightarrow c) + (s \rightarrow c)$ is normalized to 1. This agrees very well with the observed number of 1.35 ± 0.24 . However, a note of caution is in order because the value for η_s used in this calculation was measured in experiments with a higher Q^2 than this experiment. Conversely, it is reassuring to note that the number of strange particles per μ^-e^+ event arising from charm is relatively insensitive to η_s . For example, reducing η_s by a factor of 2 only lowers the expected number of strange particles per μ^-e^+ event to 1.3. So, in the spirit of a consistency check, the expected number of neutral strange particles per μ^-e^+ event from charm agrees with that observed.

D. Charm production

The predominant source of ν -induced dileptons is the production and subsequent semileptonic decay of charmed particles. Therefore, a dilepton sample is an enhanced source of charm that provides a good sample with which to study the production of charm by neutrinos. However, because of a combination of a lack of knowledge of the semileptonic branching ratios for charmed particles and limited statistics, previous experiments examining μ^-e^+ production have not been very successful in establishing the production rates for specific

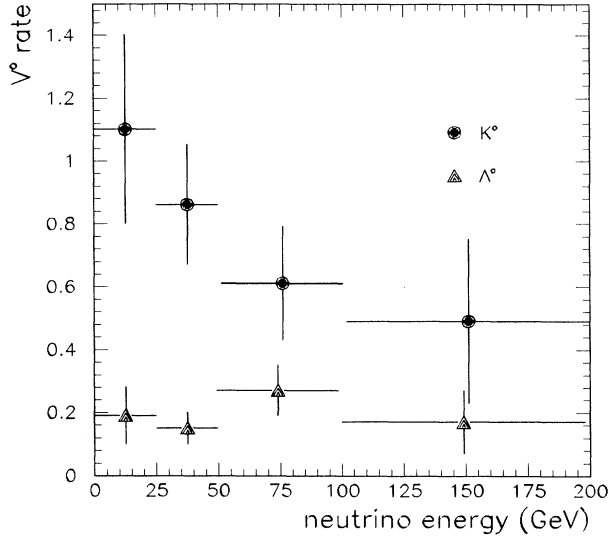


FIG. 8. Corrected number of neutral strange particles per μ^-e^+ event as a function of the incident neutrino energy.

charmed-particle final states in neutrino interactions. Fortunately, recent e^+e^- experiments have reported measurements of some of the necessary branching ratios. Also, E53 has roughly an order of magnitude more data than any previous experiment examining μ^-e^+ events in a bubble chamber. So, a reasonable derivation of the Λ_c^+ , D^0 , and D^+ production rates is now possible.

1. Invariant-mass distributions

The Λ^0e^+ and $K_S^0e^+$ invariant-mass distributions are shown in Figs. 9 and 10, respectively. The solid lines show all the combinations and the shaded region shows only those events with $P_{e^+} > 4$ GeV/c. As expected, most of the Λ^0 's and K 's are consistent with being from charm decays, i.e., $m(\Lambda^0e^+) < m(\Lambda_c^+)$ and $m(K_S^0e^+) < m(D)$.

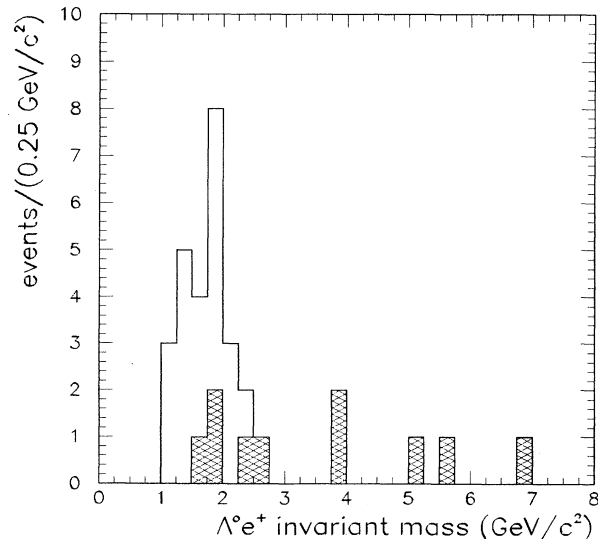


FIG. 9. Invariant-mass distribution for Λ^0 and e^+ . The solid line gives all combinations. The shaded region shows only those combinations in which $P_{e^+} > 4$ GeV/c.

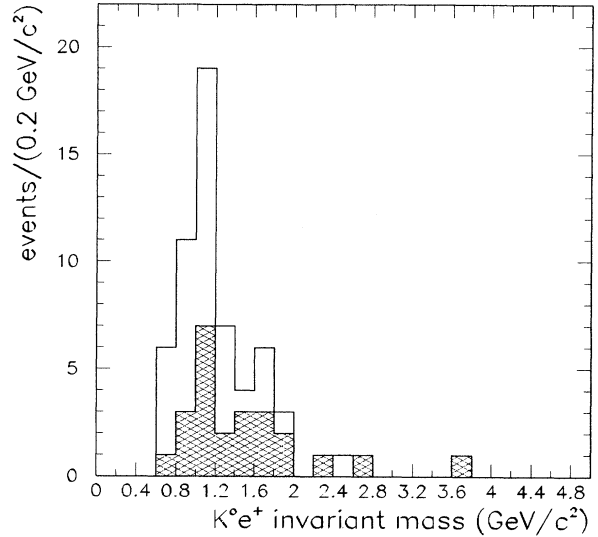


FIG. 10. Invariant-mass distribution for K_S^0 and e^+ . The solid line gives all combinations. The shaded region shows only those combinations in which $P_{e^+} > 4$ GeV/c.

It is notable that most of the Λ^0 events with $P_{e^+} > 4$ GeV/c have effective masses larger than the Λ_c^+ mass. This is not true for the corresponding meson decays. This suggests that the positrons from charmed-baryon decays are softer than those from charmed mesons. The effect of this can be seen in the results of opposite-sign dimuon bubble-chamber experiments. In this case there is a high-momentum cut ($P_\mu > 4$ GeV/c) on the second lepton and a low- Λ^0 production rate is reported.¹⁴

2. Λ_c^+ production

As stated in Sec. V C there are 31 Λ^0 's observed in 461 μ^-e^+ events. Of these Λ^0 's, five have an $e^+\Lambda^0$ invariant mass that is much larger than the Λ_c^+ mass. After removing these events and correcting for cuts and efficiencies (as done in earlier work) this leaves 62 ± 15 Λ^0 's that are consistent with those coming from semileptonic Λ_c^+ decays. Assuming all of these Λ^0 's come from Λ_c^+ decays, it is possible to calculate the total number of Λ_c^+ 's produced in the experiment by dividing the number of Λ^0 's by $B(\Lambda_c^+ \rightarrow e^+\Lambda^0 X)$. Vella *et al.* measured this branching ratio to be $(1.1 \pm 0.8)\%$ using the Mark II detector at the SLAC e^+e^- storage ring SPEAR.²⁰ This yields a value of 5600_{-2700}^{+15100} Λ_c^+ 's produced in this experiment. Dividing this by the total number of ν_μ charged-current events in the experiment gives a Λ_c^+ production rate of

$$\frac{\nu_\mu \text{Ne} \rightarrow \mu^- \Lambda_c^+ X}{\nu_\mu \text{Ne} \rightarrow \mu^- X} = \frac{5600_{-2700}^{+15100}}{146700 \pm 11700} = (4_{-2}^{+10})\% .$$

This rate calculation makes use of the assumption that most of the Λ^0 's in this sample come from Λ_c^+ semileptonic decays. Naively one might also expect $e^+\Lambda^0$ combinations to come from decays of B mesons or heavier

charmed baryons. The CLEO and ARGUS Collaborations have shown that in B -meson decays to a final state including a Λ^0 , the Λ^0 generally comes from a Λ_c^+ intermediate state.²¹ Any $e^+\Lambda^0$ events that come from a heavy charmed baryon that does not cascade down through a Λ_c^+ tend to increase the production ratio derived above. Therefore, conservatively one should regard the reported rate as an upper limit to the real value. It should also be noted that the number of Λ_c^+ 's used in this rate calculation is uncorrected for the 300-MeV/ c momentum cut on the positron. This correction is negligible compared to the uncertainty in the overall number of Λ_c^+ 's that comes from the error in $B(\Lambda_c^+ \rightarrow e^+\Lambda^0 X)$.

3. D production

The D^0 and D^+ production-rate calculations are more complicated than that for the Λ_c^+ . Two methods were used to derive the D production rates from the μ^-e^+ data. Because the methods involved slightly different assumptions they are presented separately and referred to as methods I and II.

Method I depends on the number of μ^-e^+ events in the experiment. All the μ^-e^+ events are assumed to come from Λ_c^+ , D^0 , or D^+ semileptonic decays in charged-current ν_μ interactions. This ignores the contribution from semileptonic decays of the D_s^+ . This contribution is negligible. The total D_s^+ production rate in ν_μ interactions has been measured to be small (roughly 6% of the production of D^0 and D^+).²² Also, the semileptonic branching ratio of the D_s^+ is expected to be small because the measured lifetime of the D_s^+ is about the same as the D^0 .²³ This method also ignores the possibility of μ^-e^+ events arising from the semileptonic decay of B mesons or heavy charmed baryons (other than the Λ_c^+).

The number of μ^-e^+ events arising from Λ_c^+ decays was estimated from

$$\mu^-e^+|_{\Lambda_c^+} = (\Lambda_c^+)B(\Lambda_c^+ \rightarrow e^+X),$$

where (Λ_c^+) is the number of Λ_c^+ 's produced in the experiment and $\mu^-e^+|_{\Lambda_c^+}$ is the number of μ^-e^+ events arising from Λ_c^+ production and subsequent semileptonic decay. Taking the number of Λ_c^+ to be 5600_{-2700}^{+15100} and $B(\Lambda_c^+ \rightarrow e^+X) = (4.5 \pm 1.7)\%$ as measured by Vella *et al.*,²⁰ the number of μ^-e^+ events from Λ_c^+ decays is 252_{-198}^{+763} . Subtracting this from the total of 618 ± 74 μ^-e^+ events in the experiment leaves 366_{-766}^{+211} events arising from D^0 and D^+ decays. The total number of μ^-e^+ events coming from D decays can be expressed in terms of the total number of D^0 's and D^+ 's produced in the experiment by using the measured semileptonic branching ratios of the D 's:¹⁹

$$\begin{aligned} \mu^-e^+|_D &= \mu^-e^+|_{D^0} + \mu^-e^+|_{D^+}, \\ \mu^-e^+|_D &= (D^0)B(D^0 \rightarrow e^+X) + (D^+)B(D^+ \rightarrow e^+X), \\ 366_{-766}^{+211} &= (D^0)(7.7 \pm 1.10)\% + (D^+)(19.2_{-1.6}^{+2.3})\%. \end{aligned}$$

The notation used here is similar to that used at the start of the paragraph. Using the measured result for the pro-

duction ratio of D^0 to D^+ in charged-current ν_μ interactions,²²

$$\frac{\sigma(D^+)}{\sigma(D^0)} = 0.7 \pm 0.2,$$

the number of D^0 's produced in the experiment is calculated to be 1740_{-3690}^{+1160} . Similarly the number of D^+ 's is 1220_{-2560}^{+720} . These numbers yield production rates per charged-current ν_μ event of $(1.2_{-2.5}^{+0.8})\%$ and $(0.8_{-1.7}^{+0.5})\%$ for D^0 's and D^+ 's, respectively. Within the accuracy of this experiment any correction for the low 300-MeV/ c cut on the e^+ momentum is negligible.

Method II uses the number of K^0 's produced in the μ^-e^+ events rather than the number of μ^-e^+ events to calculate the D^0 and D^+ production rates. Three of the observed K_S^0 's were removed from the K_S^0 sample prior to the calculation because of the improbability that they arose from semileptonic charmed-particle decays. In one event the $K_S^0 e^+$ invariant mass was much larger than the mass of the Λ_c^+ . In the other two there were two V^0 's in each event. One had a K_S^0 and a Λ^0 . This event was taken as a Λ^0 event in these calculations. In the other there were two K_S^0 's. This event was taken to be a single K_S^0 event. This leaves a total of 57 ± 8 observed K_S^0 's that are appropriate to use in this calculation. Correcting this number for cuts, branching ratios, and efficiencies (as done in Sec. V C) gives 286 ± 40 K^0 's.

For method II the 286 ± 40 K^0 's produced in the 461 μ^-e^+ events are assumed to come from Λ_c^+ , D^0 , or D^+ decays. The number of K^0 's from Λ_c^+ decays is obtained from

$$K^0|_{\Lambda_c^+} = (\Lambda_c^+)B(\Lambda_c^+ \rightarrow e^+K^0X).$$

Unfortunately, $B(\Lambda_c^+ \rightarrow e^+K^0X)$ has not been measured. Assuming the validity of the simplest spectator diagrams for Λ_c^+ decay into a strange meson and a nonstrange baryon, it is possible to estimate $B(\Lambda_c^+ \rightarrow e^+K^0X)$ from the measured value of $B(\Lambda_c^+ \rightarrow e^+pX) = (1.8 \pm 0.9)\%$:²⁰

$$\begin{aligned} B(\Lambda_c^+ \rightarrow e^+K^0X) &= (0.95) \times (0.5 \pm 0.2)F \\ &= (0.5 \pm 0.5)\%, \end{aligned}$$

where

$$F = B(\Lambda_c^+ \rightarrow e^+pX) - B(\Lambda_c^+ \rightarrow \Lambda^0 X)B(\Lambda^0 \rightarrow \pi p).$$

The factor of 0.95 is the Cabibbo-favored probability that there be a strange particle in the final state. The factor of 0.5 ± 0.2 is an estimate of the ratio

$$\frac{B(\Lambda_c^+ \rightarrow e^+nX)}{B(\Lambda_c^+ \rightarrow e^+pX)}.$$

This value was chosen after examining the results of four different theoretical calculations of this ratio.²⁴ F is the inclusive branching ratio for Λ_c^+ 's into protons excluding protons from $\Lambda_c^+ \rightarrow \Lambda^0 \rightarrow p\pi$. The values for $B(\Lambda_c^+ \rightarrow \Lambda^0 X)$ and $B(\Lambda^0 \rightarrow \pi p)$ used to calculate F were $(1.1 \pm 0.8)\%$ (Ref. 20) and 64.1% (Ref. 19), respectively.

Using the corrected value for $B(\Lambda_c^+ \rightarrow e^+K^0X) = (0.5 \pm 0.5)\%$ and the number of Λ_c^+ 's produced in the

TABLE V. Summary of charmed-particle production rates integrated over the incident neutrino spectrum.

Rate	E53	E531	SKAT
$\frac{\nu_\mu \text{Ne} \rightarrow \mu^- \Lambda_c^+ X}{\nu_\mu \text{Ne} \rightarrow \mu^- X}$	$(4^{+10}_{-2})\%$	$(0.8^{+0.4}_{-0.2})\%$	$(6.7 \pm 3.5)\%$
$\frac{\nu_\mu \text{Ne} \rightarrow \mu^- D^0 X}{\nu_\mu \text{Ne} \rightarrow \mu^- X}$	$(1.7^{+0.5}_{-0.7})\%$	$(2.4 \pm 0.4)\%$	$D^0 + D^+$
$\frac{\nu_\mu \text{Ne} \rightarrow \mu^- D^+ X}{\nu_\mu \text{Ne} \rightarrow \mu^- X}$	$(1.3^{+0.4}_{-0.5})\%$	$(1.7^{+0.3}_{-0.6})\%$	$(2.5 \pm 0.9)\%$

experiment (5600^{+15100}_{-2700}) gives 28^{+81}_{-31} as the number of K^0 's produced by Λ_c^+ decays in the $\mu^- e^+$ sample. The total number of K^0 's produced in D decays is obtained by subtracting those produced by Λ_c^+ decays from the total. This, in turn, can be related to the number of D^0 's and D^+ 's by using $B(D^0 \rightarrow e^+ K^0 X)$ and $B(D^+ \rightarrow e^+ K^0 X)$:

$$K^0|_D = K^0|_{\text{total}} - K^0|_{\Lambda_c^+} = (286 \pm 40) - (28^{+81}_{-31}) \\ = (258^{+51}_{-90}),$$

$$K^0|_D = K^0|_{D^0} + K^0|_{D^+},$$

$$K^0|_D = (D^0)B(D^0 \rightarrow e^+ K^0 X) \\ + (D^+)B(D^+ \rightarrow e^+ K^0 X).$$

The values for $B(D^0 \rightarrow e^+ K^0 X)$ and $B(D^+ \rightarrow e^+ K^0 X)$ are estimated by

$$B(D^0 \rightarrow e^+ K^0 X) = \frac{1}{2}(0.95)B(D^0 \rightarrow e^+ X)$$

and

$$B(D^+ \rightarrow e^+ K^0 X) = \frac{1}{2}(0.95)B(D^+ \rightarrow e^+ X).$$

The factor of 0.95 is the Cabibbo-favored probability of a strange particle occurring in the final state and the factor of $\frac{1}{2}$ comes from the requirement that the kaon in the final state be neutral. Using the world-average values for the measured branching ratios,¹⁹ $B(D^0/D^+ \rightarrow e^+ X)$, gives $(3.7 \pm 0.7)\%$ and $(9.1 \pm 1.8)\%$ for $B(D^0 \rightarrow e^+ K^- X)$ and $B(D^+ \rightarrow e^+ K^0 X)$, respectively. The relative errors in these quantities have been increased to 20%. This is because the relative error in the estimated quantities should be larger than those in the measured quantities. Folding in these numbers with the measured D^0 -to- D^+ production ratio²² gives a value of 2550^{+770}_{-1060} for the number of D^0 's produced in this experiment. The calculated number of D^0 's per charged-current ν_μ event is $(1.7^{+0.5}_{-0.7})\%$. The comparable numbers for D^+ production are 1840^{+540}_{-750} and $(1.3^{+0.4}_{-0.5})\%$, respectively.

Although the two methods are not completely independent, it is gratifying to note that the numbers calculated using method II are consistent with those calculated using method I. The errors using method II are smaller be-

cause this method depends to a lesser degree on the value of $B(\Lambda_c^+ \rightarrow e^+ \Lambda^0 X)$ which has a large error.

Table V summarizes the results of the calculations of charmed-particle production rates for this experiment. Results from E531 and SKAT are given for comparison.^{22,25} These rates agree very well with those derived in this experiment.

VI. CONCLUSIONS

In this paper the characteristics of neutrino-induced $\mu^- e^+$ dilepton events are studied. The 461 $\mu^- e^+$ events making up the data sample for this experiment represent roughly an order-of-magnitude increase in statistics over any previous similar experiment. A careful analysis of the final states of these events is possible because the data were taken using a bubble chamber. The importance of this work is enhanced with the recent decommissioning of the 15-ft bubble chamber at Fermilab, which marked the end of experiments doing relatively-high-statistics studies of neutrino interactions in bubble chambers.

The results presented here support the well-established hypothesis that $\mu^- e^+$ dilepton events arise from the production and subsequent semileptonic decay of charmed particles. The overall and energy-dependent rates for $\mu^- e^+$ production observed in this experiment are very similar to those reported in previous experiments. The expected enhancement of strange-particle production in these events is seen. In addition, neutrino production rates for Λ_c^+ , D^0 , and D^+ are derived using two different methods. The observed rates are consistent with results reported by other experiments.

ACKNOWLEDGMENTS

We thank the scanning and measuring staffs at our institutions, as well as the operating crews of the 15-ft bubble chamber and the neutrino beam at Fermilab. One of us (S.M.) thanks Professor M. Shaevitz for several helpful discussions. This research was supported by the U.S. Department of Energy and by the National Science Foundation.

- *Present address: Bear, Stearns, and Co., Inc., New York, NY 10167.
- †Present address: Yale University, New Haven, CT 06511.
- ‡Present address: Adelphi University, Garden City, NY 11530.
- §Permanent address: Seton Hall University, South Orange, NJ 07079.
- ¹N. J. Baker *et al.*, Phys. Rev. D **32**, 531 (1985).
- ²A. Benvenuti *et al.*, Phys. Rev. Lett. **34**, 419 (1975).
- ³A. Benvenuti *et al.*, Phys. Rev. Lett. **41**, 1204 (1978); M. Jonker *et al.*, Phys. Lett. **107B**, 241 (1981); H. Abramowicz *et al.*, Z. Phys. C **15**, 19 (1982); K. Lang *et al.*, *ibid.* **33**, 483 (1987); C. Foudas *et al.*, Phys. Rev. Lett. **64**, 1207 (1990).
- ⁴H. Deden *et al.*, Phys. Lett. **67B**, 474 (1977); N. Armenise *et al.*, *ibid.* **86B**, 115 (1979); H. C. Ballagh *et al.*, Phys. Rev. D **21**, 569 (1980); **24**, 7 (1981); A. Haatuft *et al.*, Nucl. Phys. **B222**, 365 (1983); V. V. Ammosov *et al.*, Z. Phys. C **35**, 329 (1987); V. Jain *et al.*, Phys. Rev. D **41**, 2057 (1990).
- ⁵TVGP and SQUAW were originally written by the Alvarez group at Berkeley. See F. T. Solmitz *et al.*, LBL Alvarez Group Programming Note P-117, 1966 (unpublished). For details on adaptation for use with the 15-ft bubble chamber, see E. E. Schmidt, Jr., Nevis Report No. 224, Ph.D. thesis, Columbia University, 1978.
- ⁶S. Manly, Nevis Report No. 268, Ph.D. thesis, Columbia University, 1988; N. J. Baker *et al.*, Phys. Rev. D **41**, 2653 (1990).
- ⁷A. Buras and K. J. B. Gaemers, Nucl. Phys. **B132**, 249 (1978); A. Buras, *ibid.* **B125**, 125 (1977); A. De Rújula *et al.*, *ibid.* **B154**, 394 (1979). This code was obtained from C. Foudas of the Chicago-Columbia-Fermilab-Rochester (CCFR) Collaboration.
- ⁸J. Liu, Nevis Report No. 255, Ph.D. thesis, Columbia University, 1985.
- ⁹Manly (Ref. 6); S. Manly, C. Baltay, and M. Kalelkar, Nucl. Instrum. Methods **A290**, 393 (1990).
- ¹⁰H. Georgi and H. D. Politzer, Phys. Rev. D **14**, 1829 (1976); R. M. Barnett, *ibid.* **14**, 70 (1976); A. De Rújula *et al.*, Rev. Mod. Phys. **46**, 391 (1974).
- ¹¹H. Abramowicz *et al.*, Z. Phys. C **15**, 19 (1982).
- ¹²K. Lang *et al.*, Z. Phys. C **33**, 483 (1987).
- ¹³H. C. Ballagh *et al.*, Phys. Rev. D **24**, 7 (1981).
- ¹⁴N. Armenise *et al.*, Phys. Lett. **86B**, 115 (1979).
- ¹⁵C. Foudas *et al.*, Phys. Rev. Lett. **64**, 1207 (1990).
- ¹⁶A. Benvenuti *et al.*, Phys. Rev. Lett. **41**, 1204 (1978).
- ¹⁷M. Jonker *et al.*, Phys. Lett. **107B**, 241 (1981).
- ¹⁸N. J. Baker *et al.*, Phys. Rev. D **34**, 1251 (1986).
- ¹⁹Particle Data Group, G. P. Yost *et al.*, Phys. Lett. B **204**, 1 (1988).
- ²⁰E. Vella *et al.*, Phys. Rev. Lett. **48**, 1515 (1982).
- ²¹M. S. Alam *et al.*, Phys. Rev. Lett. **59**, 22 (1987); H. Albrecht *et al.*, Z. Phys. C **42**, 519 (1989).
- ²²N. Ushida *et al.*, Phys. Lett. B **206**, 375 (1988).
- ²³G. H. Trilling, Phys. Rep. **75**, 57 (1981).
- ²⁴E. Vella *et al.*, Phys. Rev. Lett. **48**, 1515 (1982); S. R. Klein, Int. J. Mod. Phys. A **5**, 1457 (1990).
- ²⁵V. V. Ammosov *et al.*, Z. Phys. C **35**, 329 (1987).